Elsa Pacciani

Anthropological description of skeletons from graves no. 123, 124, 125, 126, 127, 128, 129, 130, 131, 132, 133, 134, 135, 136, 141, 142, 143, 145 and 146 at Skriðuklaustur Monastery

Skýrslur Skriðuklaustursrannsókna XXVIII

Elsa Pacciani

Anthropological description of skeletons from graves no. 123, 124, 125, 126, 127, 128, 129, 130, 131, 132, 133, 134, 135, 136, 141, 142, 143, 145 and 146 at Skriðuklaustur Monastery

Anthropological description
of skeletons from graves no. 123, 124, 125, 126, 127, 128, 129, 130, 131, 132, 133, 134, 135, 136, 141, 142, 143, 145 and 146 at Skriðuklaustur Monastery
Vala Gunnarsdóttir bjó til prentunar
Skýrslur Skriðusklaustursrannsókna XXVIII
Útgefandi: Skriðuklaustursrannsóknir og Soprintendenza per i Beni Archeologici della Toscana, Italy
Útgáfustaður: Reykjavík

Forsíðumynd: A femur from grave 130. Shows a healed fracture.

ISBN 978-9979-9970-6-1
ISSN 1670-7982

Table of contents

Introduction

This description was made “on the field”, soon after the excavation, the preliminary cleaning and restoration. Thus, its aim is mostly to record the identifying data and some relevant observations, thereby offering cues, research lines and suggestions for widening of particular aspects.

So there is no pretence of exhaustiveness, as the anthropological study requires more time and the simultaneous disposability of the whole sample, for screening and comparisons about the various characters. Moreover many features need to be examined by lab specific tools and equipping. However some generalities, observations and statements can be related here:

A marked sexual dimorphism characterizes this sample and makes the sex diagnosis relatively easy, together with the good state of preservation; very few cases raised some uncertainty. So a morphological diagnosis was performed, on the basis of the most discriminant hip bone and skull features, and taking into account also the other bones. No sex diagnosis was attempted on subadults.

About the age-at–death diagnosis I decided to avoid a subdivision of adult individuals in small age classes, because of the weakness of all the aging indicators due to the high individual and population variability. For this reason I adopted a gross subdivision in three classes: young adult (conventionally beginning from the spheno-occipital suture closure or the third molars eruption), mature adult and old adult, on the basis of a complex of traits appearance, such as pubic symphysis, auricular surface, dental wear and pathology, cranial suture closure, joint degeneration, spongy bone rarefaction etc.. A more precise diagnosis will be possible when the whole sample will be examined in order to detect the “population” aging rate, or /and other traits will be examined, such as dental cement anulation, pulp/tooth ratio etc.

For dental wear quantification I used the Lovejoy 1985 graphic scheme which represents phases of maxilla and mandible wear, but without attributing the specimens to the associated age classes, because I have found, in my previous methodological research, a huge divergence between the Lovejoy age classes and the real age. As aging methods I adopted:

- for the pubic symphysis, Brooks and Suchey 1990 scale
- for the auricular surface, Lovejoy et al 1985 scale
- for the sternal end of the ribs, Iscan et al 1984 scale

Subadult age-at–death diagnosis was made according the Ubelaker (1989) dental development standard.

A restricted selection of measurements was made with a purely identifying aim regarding the skull, and with the purpose of underscoring some stress indicators and anthropological conditions (stature, robusticy, platymeria, platicnemia) regarding the postcranial bones. In measuring pair bones, I chose the best preserved side; when sides were equally preserved, I chose the left one; when I detected a clear asymmetry, I reported it in the text.

Of course it will be possible and advisable to take a much larger amount of measurements in the anthropology laboratory, where having the availability of all the necessary anthropometric instruments and, above all, having specific finalities in an organic research project.

The dental formula is presented for each individual in a table, whose legend is the following:

P = present
AM = lost ante mortem
PM = lost postmortem
AG = genetically absent
R = root only
NE = not erupted
- - = not detectable

The stature was calculated by the formulas of Olivier et al. 1978, based on the physiologic lenght of the femur (n. 2 according Martin and Saller).

Degree of resorption of alveolar bone, due to periodontal disease is attributed according to the simple scale of Brothwell 1981 (No alveolar destruction; Slight, Medium, Considerable).

The same author was followed for the degree of calculus formation (Slight, Medium, Considerable). Diastema is a gap or space between two teeth. It happens when there is an unequal relationship between the size of the teeth and the jaw.

A very peculiar and interesting pathologic condition is recurrent in the sample and requires an accurate analysis and a differential diagnosis. Even 5 individuals (see the single descriptions below), out of 13 adults in this group exhibit the characteristic signs: the distal epiphyses of some long bones appear “swollen” and show porosity, erosion, pitted surface, new bone apposition, while other long bones appear normal. Hand bones are the most affected, with a “swollen” look and lytic lesions: holes, erosions and pits. Also the joint surfaces appear altered, with erosion areas, deformation and osteophytosis.

Another group characteristic is the high frequency of Echinococcus cysts: even 4 individuals are affected.

Anthropological description 2009

Grave 123

Fig. 123.1

Sex: Uncertain. Some features are masculine: inion, absence of frontal eminences, mastoid process, square chin, ulna and fibula well shaped for muscle attachments; other feature are feminine: supraorbital edge, gonion, glabella, mandibular condyle.

Age at death: Mature adult.

Dental wear is low: degree E for posterior teeth; degree B2 for anterior ones. But cranial sutures are partly closed: lateral parts of the coronal, almost all the sagittal, some portion of the lambdoid.

Stature: Not detectable.

Dental characteristics:

	Right								Left							
	M3	**M2**	**M1**	**P2**	**P1**	**C**	**I2**	**I1**	**I1**	**I2**	**C**	**P1**	**P2**	**M1**	**M2**	**M3**
Maxilla	--	--	--	--	--	--	--	--	--	--	--	--	--	--	--	--
Mandibula	P	P	P	P	P	P	P	P	P	P	P	P	P	P	P	P

- Malocclusion: left P2 dislocated lingually.
- Caries no.
- Periodontitis (phase: Medium) (Fig. 123.2).
- Calculus (phase: Medium).

Fig. 123.2

Fig. 123.3

Occupational stress indicators and pathological aspects:

The few bones better preserved show signs of activity: ulna diaphysis, fibula, metacarpals. The first right metacarpal shows enthesopathy of the muscle opponens pollicis.

Occipital condyles are affected by marginal osteophytosis. Besides they are asymmetric: the left one is flattened, the right one shows an accessory facet in lateral-posterior position (Fig.123.3). Moreover, the occipital foramen has an asymmetric shape. Atlas can give an explanation about that: it is lacking of the right arm of the posterior arch, because of a congenital defect (Fig.123.4). The anomaly has repercussions on C2 and C3, which show asymmetric shape of the intervertebral facets and anterior shortening of the bodies (Fig.123.5, 123.6).

Fig. 123.4

Fig. 123.5

Fig. 123.6

Another consequence is the temporo-mandibular arthritis, bilateral and asymmetric: on the right side, flattening and enlargement of the fossa mandibularis and an area of bony buildup (Fig.123.7); on the left side, the formation of an accessory facet (Fig.123.8).

Other observations: trace of metopism: a little (1 cm) segment close to the naso-frontal suture.

Os acromiale not detectable for incompleteness.

Fig. 123.7

Fig. 123.8

Grave 124

Sex: Female (small mandible, sharp supraorbital edge, small humerus dimensions).

Age at death: Adult (weared M3) young (frontal suture completely open, dental wear: maxillary degree C; mandibular degree D).

Dental characteristics:

Fig. 124.1

	Right								Left							
	M3	**M2**	**M1**	**P2**	**P1**	**C**	**I2**	**I1**	**I1**	**I2**	**C**	**P1**	**P2**	**M1**	**M2**	**M3**
Maxilla	P	P	P	--	--	P	P	P	P	P	P	P	P	P	P	--
Mandibula	P	P	P	P	P	P	P	P	PM	P	P	P	P	P	P	PM

- Hypoplasia striae on central incisors, canines and premolars.
- No shovel shape incisors.
- No caries.
- Calculus: Medium.
- Periodontitis: absent.
- Incisors have fractured edge (Fig.124.2, 124.3); upper right M1 has fractured disto-lingual cusp (Fig.124.4).

Fig. 124.2

Fig. 124.3

Fig. 124.4

Grave 125

Only lower limbs are present.

Sex: Male (femur head and condyles dimensions).

Age at death: Mature adult (slight arthritis signs at the at the femur head and knee joints).

Stature: Cm 160.

Occupational stress indicators and pathological aspects:

On femurs: enthesopathies of the ligament of the head (Fig.125.2) and gluteus maximus (Fig.125.3).

Fig. 125.1

Arthritis signs at the head: marginal osteophytosis and endoarticular neoapposition (Fig. 125.2) and at the knee joint. Platimeria.

Both tibiae show periostitis all over the diaphysis, and vascular imprints on the antero-lateral face (Fig.125.4). Also the fibulae are periostitic.

The right fibula is curved, with medial convessity (Fig.125.5, 125.6) causing twisted relations and osteophytosis at the ankle joint (Fig 125.7), and osteophytosis at the foot joints, in particular the right first metatarsal (Fig 125.8, 125.9) and first phalanx (Fig. 125.10). The whole foot trim is altered. Also the soleus muscle attachment on the right tibia is more expressed than left, indicating an anomalous deambulation (Fig.125.11).

Fig. 125.2

Fig. 125.3

Both patellae show the quadriceps tendon enthesopathy (Fig. 125.12).

Fig. 125.4

A scattered right femur and rotula are included in the box, not belonging to this individual (the excavator says they could be matched with the articulated individual of grave 140). It is well preserved, except some exfoliation of the diaphysis and extremities erosion. It shows a slight marginal osteophytosis at the knee articulation (Fig.125.13).

The **stature** of the individual is cm 173.

Fig. 125.5

Fig. 125.6

Fig. 125.7

Fig. 125.8

Fig. 125.9

Fig. 125.10

Fig. 125.11

Fig. 125.12

Fig. 125.13

Grave 126

Fig. 126.1

Fig. 126.2

Sex: Female (morphological diagnosis, on the basis of the most discriminant cranial and hip bone features).

Age at death: Mature, on the basis of dental wear (phase G on maxilla, H on mandible), according to the scale of Lovejoy, 1985), auricular surface (degree 7) sternal ends of the ribs and arthritis signs; even if cranial sutures are completely open.

Stature: Cm 154.

Dental characteristics:

	Right								Left							
	M3	**M2**	**M1**	**P2**	**P1**	**C**	**I2**	**I1**	**I1**	**I2**	**C**	**P1**	**P2**	**M1**	**M2**	**M3**
Maxilla	P	AM	P	P	R	P	P	P	P	P	P	P	P	P	P	P
Mandibula	P	P	P	P	P	P	P	AM	R	P	P	P	P	P	P	P

An abscess is located in correspondence with upper right M2, lost. A second one is in correspondence with lower right M1, which is fractured in the proximal side (Fig. 126.3, 126.4).

Periodontitis : Considerable.

Calculus: Considerable.

Fig. 126.3

Caries absent.

A diastema is located between upper left M3 and M2.

Malocclusion absent.

Shovel shaped incisors.

Fig. 126.4

Fig. 126.5

Occupational stress indicators and pathological aspects:

The deltoid muscle attachments are enthesopathic on both clavicles and very developed on both humeri (Fig.126.5); also the the pectoralis major (Fig 126.6) and teres major (Fig. 126.7) are very developed and enthesopathic as well as the brachiradialis (Fig. 126.8).

The ulnae and radii show marked insertions of flexors and extensors on the diaphysis, besides the biceps. Hands show sharp edges on metacarpals for dorsal and palmar interossei, and exceptionally developed insertions for flexor digitorum muscles (Fig. 126.9). As this complex of stress indicators is bilateral and involves the deltoid (abductor muscle) and the flexion/extension muscles, we can imagine an explaining activity such as laundress. The right ulna shows also enthesopathic insertions of brachialis and pronator quadratus.

Fig. 126.6

Fig. 126.7

Fig. 126.8

Arthritis signs (marginal osteophytosis) are visible on humeral head (Fig. 126.10), elbow, wristle, carpals and metacarpals , confirming a stressing activity of upper limbs.

Platimeria.

Bilateral acetabulum arthritis.

Marked bilateral superior tibiofibular joint arthritis (Fig. 126.11).

“Squatting” facets on the anterior edge of the ankle joint.

Ankylosis between the first and second phalanx of the third finger, of traumatic origin. (Fig. 126.12).

Dorsal extension of the first metatarsal distal joints (Fig. 126.13). Severe arthritis (porosity, enlargement) on the left intervertebral facets of C4-C5 and C7-T1 (Fig 126.14, 126.15). Slight arthritis on the cervical and thoracic segments of the column.

Radio and ulna lengths denote asymmetry of the upper limbs (radio max. length: right mm 215, left mm 211; ulna max. length: right mm 231, left mm 227). Left humerus is not measurable.

A deep preauricular sulcus indicates pregnancies.

Echinococcus cyst (a parasitic infection which affects people who herd sheep using dogs) of huge dimensions was found in the liver region (Fig.126.16).

Other observations: Os acromiale not detectable. Presence of torus palatinus.

Fig. 126.9

Fig. 126.10

Fig. 126.11

Fig. 126.12

Fig. 126.13

Fig. 126.14

Fig. 126.15

Fig. 126.16

Loose bones in grave 126:

Some skull fragments

1 mandible, lacking teeth (most of them lost in life, at least all molars) and rami.

2 controlateral humerus diaphyses

2 controlateral ulna diaphyses

2 controlateral mastoid processes

2 controlateral femur diaphyses

2 controlateral tibia diaphyses

fragment of scapula, hip bone, ribs, hands and feet

All the bones can belong to a female individual, characterized by little build, and rather old age.

Grave 127

Fig. 127.1

Fig. 127.2

Age at death: Newborn, on the basis of teeth development (Fig. 127.2).

Very fragmentary remains. The skull (squama fragments, pyramids, left orbit, basis) and most of the postacranial bones are represented: right clavicle, right and left ribs, vertebrae, humeri, forearms, hip bones, femurs, tibiae, fibulae, right hand (10 elements), left hand (9 elements, right foot (5 elements), left foot (2 elements). The bones are incomplete and curled up. The presence of some tooth crowns allows us to determinate the age at death, coincident with the birth.

Dental characteristics:

	right					**left**				
	m2	**m1**	**c**	**i2**	**i1**	**i1**	**i2**	**c**	**m1**	**m2**
Maxilla	**P**	**--**	**--**	**P**	**P**	**P**	**P**	**P**	**P**	**P**
Mandibula	**--**	**--**	**--**	**--**	**--**	**--**	**--**	**--**	**--**	**--**

Grave 128

Fig. 128.1

Fig. 128.2

Sex: Female (morphological diagnosis, on the basis of the most discriminant cranial and hip bone features).

Age at death: Old:

Advanced dental wear, exceeding the maximum degree of the Lovejoy scale.

Cranial sutures in advanced closure.

Presence of osteoporosis.

Presence of diffuse arthritis.

Pubis symphysis: degree 4.

Auricular surface: very porotic, irregular edges, retroauricular activity traces (phase 8).

Dental characteristics:

	Right								Left							
	M3	**M2**	**M1**	**P2**	**P1**	**C**	**I2**	**I1**	**I1**	**I2**	**C**	**P1**	**P2**	**M1**	**M2**	**M3**
Maxilla	AG	P	P	P	P	P	P	P	P	P	P	P	P	P	P	AG
Mandibula	AG	P	P	P	AM	P	P	AM	AM	P	PM	R	AM	P	AM	AG

Periodontal disease: considerable.

Calculus: considerable.

4 diastemas on maxilla: right P1-C; right I2-I1; I1-I1; left I1-I2 (Fig. 128.3).

Dental wear of incisors is huge, almost reaching the roots (Fig. 128.3).

Buccal abscess of upper right M1.

Fig. 128.3

Fig. 128.4

Fig. 128.5

Occupational stress indicators and pathological aspects:

Enthesopaties: severe on deltoid attachments on both clavicles and both humeri (Fig. 128.4, 128.5); infraspinatus and teres minor on both scapulae (Fig. 128.6) and humeri (Fig. 128.7), but mainly on the left side; triceps on scapulae (Fig. 128.8); pectoralis major and teres major are well developed on humeri, mainly on the left side.

Common extensor and extensor carpi radialis longus muscles are enthesopatic on humeri, bilaterally (Fig. 128.9). Common flexor attachments are very developed on both humeri.

Fig. 128.6

Fig. 128.7

Fig. 128.8

Particularly noticeable are the enthesopaties of biceps tuberosity on both radii (Fig. 128.10, 128.11); of brachialis and the muscles attaching on the postero-lateral face of ulnae (abductor pollicis longus; extensor pollicis longus; extensor indicis) (Fig. 128.12, 128.13, 128.14); of supinator on radii (Fig. 128.15, see the grooving imprints and entesophyties); of teres pronator on radii (Fig. 128.16); of pronator quadratus on right ulna (Fig. 128.17). Finally the flexor digitorum muscle attachments on the anterior diaphyseal surfaces of radii and ulnae are very marked (Fig. 128.10), as well as the crests on the palmar surface of the phalangeal diaphyses (Fig. 128.18).

Fig. 128.9

Fig. 128.10

Fig. 128.11

Generally, all the main arm muscles involved in abdution/addution of the arm, flexion/extension of the forearm; prono/supination of the forearm and hand grip appear subject to strong and continue stress forces.

Both scapulae show glenoid arthritis, with marginal osteophytosis and, on the right side, a forward extension of the articular surface (Fig. 128.19).

Fig. 128.12

Fig. 128.13

Fig. 128.14

Fig. 128.15

Fig. 128.16

Fig. 128.17

Fig. 128.18

Fig. 128.19

Fig. 128.20

Fig. 128.21

Fig. 128.22

Fig. 128.24

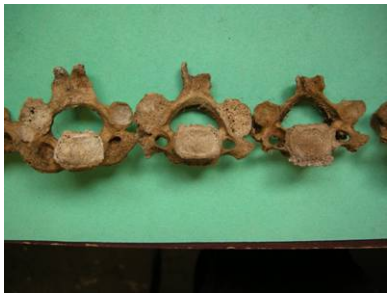

Fig. 128.25

Fig. 128.26

Fig. 128.27

This picture of extreme stress on the upper limbs can be reasonably explained by the fracture of the arch of second lumbar vertebra (see below) which undoubtedly determined the complete flaccid paralysis of both lower limbs. The woman survived the severe trauma but could not walk any more, not even on crutches, therefore we can presume that she moved on a kind of low wheeled cart, driving it by arms, possibly holding a facility tool with her hands. On the other hand, muscle enthesopaties are observable also on femurs (iliopsoas, adductor magnus, gluteus maximus, vastus medialis) and tibiae (soleus), leading to suppose alternative hypotheses of a sort of polyenthesopathy syndrome or an intense overall activity, previous the accident.

The second lumbar vertebra shows a total fracture (arch and body): the complete fracture of the arch at the peduncles, and consequent dislocation of the arch, which arranged itself obliquely, with the superior side turned backward and the inferior side forward, till leaning against the body and even burying itself in it (Fig. 128.20: superior side; Fig. 128.21: inferior side; Fig. 128.22: right side). In this way the neural channel appears completely obliterated in the lower part, indicating a very severe damage of the spinal marrow, with certain and irreversible paralysis of both lower limbs (paraplegia).

The fracture of the body (discosomatic fracture) by compression is associated, as the wedge shape (Fig. 128.22) and the imprint of the underlying vertebra on the anterior part of the lower side of the body (Fig. 128.21) show.

Fig. 128.28

Fig. 128.29

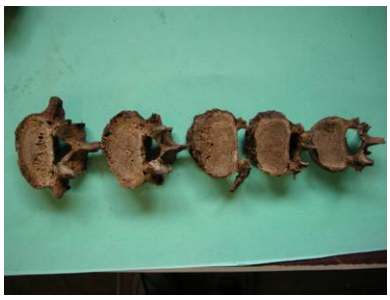

Fig. 128.30

This kind of lesion is usually due to an indirect trauma, such as a fall on own feet or behind. The vertebral colunm on the whole is affected by arthritis degeneration, mostly in consequence of the fracture of the second lumbar vertebra. The cervical segment shows severe arthritis: degenerated atlas-dens joint; scalloped and lowered bodies, especially C5and C6; some extended, irregular and porous intervertebral facets; some sclerotic, porous body and torn-edged plates (Fig. 128.24, 128.25, 128.26, 128.27). The thoracic segment appears much less affected, showing somewhat asymmetric bodies, with concave lateral surface (fish-like) only. The lumbar segment is seriously affected , with porosity of the plates, marginal

osteophytosis and lowered bodies (except L1, almost normal and L5, with porous upper plate only) (Fig. 128.28, 128.29, 128.30).

Degenerative arthritis signs are detectable on occipital condyles, temporo-mandibular joints, elbow, carpus, metacarpus.

Hand bones have a “swollen” look and lytic lesions: holes, erosions, pits (Fig. 128.31, 128.32), as other individuals of the group (see individuals N.129 ; N.130; N.143; N.145).

Other observations: Os acromiale absent, bilaterally. Metopism: initial and final short segments. Presence of torus palatinus. Presence of some small button osteomas (benign tumors) on the skull vault (Fig. 128.33). Presence of preauricular sulcus, bilaterally.

Platymeria.

Bilateral asymmetry is detectable in the humerus lengths (right mm 306, left mm 295).

Fig. 128.31

Fig. 128.32

Fig. 128.33

Grave 129

Sex: Male (morphological diagnosis, on the basis of the most discriminant cranial and hip bone features).

Age at death: old:

Advanced dental wear, exceeding the maximum degree of the Lovejoy scale; even, the whole crown is worn in almost all the maxillary teeth (Fig. 129.4, 129.5, 129.6).

Cranial sutures are open except the lateral segments of the coronal.

Auricular surface is porotic, with irregular edges and moderate traces of retroauricular activity (phase 7).

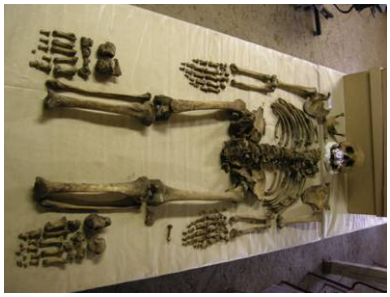

Fig. 129.1

Fig. 129.2

Fig. 129.3

Stature: Cm 160.

Dental characteristics:

	Right								Left							
	M3	**M2**	**M1**	**P2**	**P1**	**C**	**I2**	**I1**	**I1**	**I2**	**C**	**P1**	**P2**	**M1**	**M2**	**M3**
Maxilla	PM	AM	R	P	P	P	AM	P	P	P	P	P	P	R	P	P
Mandibula	P	AM	P	P	P	P	P	P	P	P	P	P	P	P	AM	P

Periodontal disease: considerable.

Six abscesses can be counted, all with a vestibular fistula:

1 – the cause of the loss of right I2 in a short time before death (alveolar edges are still sharp),

2 - a sole large abscess in correspondence of upper right M2 and M3,

3 - in correspondence of upper right M1; this tooth rotated on its lingual root (working as a swivel) and occupied the space of M2 (lost AM) with its vestibular posterior root completely raised out of the alveolus, while the vestibular anterior one is lacking (Fig. 129.7).

4 - in correspondence of upper right I2

5 - in correspondence of lower left M1; only the lingual root remains.

6 - in correspondence of lower left M2

Calculus: considerable (Fig.129.8).

Malocclusion: lower anterior teeth crowded, with vestibular dislocation of left I2 and lingual dislocation of left I1.

Fig. 129.4

Fig. 129.5

Fig. 129.6

Shovel shape incisors not detectable.

Hypoplasia not detectable.

Occupational stress indicators and pathological aspects:

Pathological aspect of the scapular glenoids, mostly on the left side: marginal osteophytes, porosity and sclerosis of the articular surface (Fig. 129.9); these signs can be associated to an impingement syndrome resulted from the presence of os acromiale (see below). An erosive area is present on the right side at the origin of the biceps tendon (Fig. 129.10); a similar erosive area is also at the sternal end of the clavicles (Fig. 129.11).

Fig. 129.7

Fig. 129.8

Fig. 129.9

Fig. 129.10

Fig. 129.11

Fig. 129.12

Fig. 129.13

Fig. 129.14

Fig. 129.15

Fig. 129.16

Fig. 129.16bis

Fig. 129.17

Fig. 129.18

Fig. 129.19

Fig. 129.20

Both humeri show evident insertions for the pectoralis major and deltoid muscles, and enthesopathies of the teres major and rotator cuff (Fig. 129.12, 129.13).

Advanced degenerative arthritis at the right elbow (Fig. 129.14). An erosive area is present on the right olecranon apex (Fig. 129.15, 129.16), on the left radial tuberosity, on the back side of both rotulae (Fig. 129.16 bis).

Fig. 129.21

Fig. 129.22

Fig. 129.23

The distal epiphyses of the right radio and ulna appear “swollen” (Fig. 129.17) and the joint surfaces appear altered too (Fig.129.18); the left one is normal.

Fig. 129.24

The same “swollen” appearance can be found on the hands: the right one, mostly at the proximal end of the second metacarpal and at the distal end of the third one (Fig. 129.19, 129.20, 129.21); the left one, even more damaged, where the carpal bones are more affected, besides the distal end of all the metacarpals and the proximal phalanges of the second and third finger (Fig. 129.22, 129.23, 129.24);. These “swollen” areas show also porosity, erosion, pitted surface, new bone apposition. This pathological condition is very similar to the one found on Individuals N. 128 and N.130.

Finally, an Echinococcus cyst was found in the right side of the abdomen(Fig. 129.25).

Fig. 129.25

Other observations: Os acromiale present bilaterally, but the non-fusion involves different ossification nuclei, so that the right acromion is shorter the the left one.

Torus palatinus absent.

Grave 130

Fig. 130.1

Fig. 130.2

Fig. 130.3

Sex: Male (morphological diagnosis, on the basis of the most discriminant cranial and hip bone features).

Age at death: Mature adult.

- Cranial sutures open except the lateral segments of the coronal.
- Dental wear advanced, exceeding the Lovejoy scale (Fig. 130.4, 130.5).
- Sternal ends of ribs in Phase 3 (Iscan et al. 1984) (Fig.130.6).
- Auricular surface of ilium: phase 5.

Stature: Cm 163.

Dental characteristics:

	Right								Left							
	M3	**M2**	**M1**	**P2**	**P1**	**C**	**I2**	**I1**	**I1**	**I2**	**C**	**P1**	**P2**	**M1**	**M2**	**M3**
Maxilla	P	P	P	P	P	P	P	p	P	P	P	AM	P	P	P	P
Mandibula	P	P	P	P	P	P	P	P	P	P	P	P	P	P	P	P

Fig. 130.4

Fig. 130.5

Fig. 130.6

Caries absent.

Periodontal disease: medium.

Abscess with buccal fistula in correspondence of upper right M1; buccal periodontal pocket in correspondence of upper right M2; buccal and lingual periodontal pockets in correspondence of upper left P1; large lingual abscess in correspondence of upper left M2.

Calculus: considerable.

3 diastemas on maxilla: right I2-I1; I1-I1; left I2-I1 (Fig. 130.4).

Malocclusion: slight rotation of lower canines.

Severe hypoplasia on lower canines; presence of striae also on other teeth, detectable despite of the abundant calculus.

Dental wear is particularly advanced on upper anterior teeth, where it is oriented obliquely, reaching the root on the lingual side.

Occupational stress indicators and pathological aspects:

The cranial vault shows multiple lesions, probably due to tertiary syphilis: gummatous pits of different width, surrounded by hyperostotic porous bone, and erosive or sclerotic areas. Four of these lesions on the frontal bone (Fig. 130.7, 130.8, 130.9) (n.1 and n.2 on the left anterior part of the squama behind the left superciliary arch, small and close to each other, oval, with the major axis in sagittal direction,; n.3, behind the right superciliary arch, larger and flatter, quadrangular shaped; n.4 on the posterior part of the squama, before the bregma, slightly on the left, grossly rounded, large and flat); four on the left parietal (Fig. 130.10, 130.11, 130.12) (n.5, the most anterior, in the corner between the coronal and sagittal sutures, is an initial erosion area; n.6, soon behind it, with irregular shape and bottom, and transversal major axis; n.7, rather flat erosion area behind n.6, close to the sagittal suture, with irregular shape and oblique major axis; n. 8, the posterior one, larger and deeper, oval, with rounded edges, rather smooth and undulated surface, transverse major axis); one on the right parietal: n.9, (Fig.130.11) the largest one, oval, sagittal major axis, rather smooth and pitted bottom, rounded edges.

The left femur distal diaphysis shows signs of gummatous and nongummatous osteoperiostitis: a large thickened area (10 cm long), mostly on the lateral side and extending to the anterior and posterior faces. The surface is rough, sieve or sclerotic, following a bony buildup process (Fig. 130.13, 130.14). In the antero-lateral side there are three grouped irregular cavities, furrowed by grooves and surrounded by porotic bone, probably corresponding to the location of gummas (Fig. 130.15, 130.16).

Tibiae are both affected by severe nongummatous osteoperiostitis. The right one shows two osteoperiostitis areas: 1) a huge thickened area with the maximum bulge mostly on the anterior margin at half diaphysis but extending to the antero-lateral and antero-medial faces on almost the whole diaphysis (Fig. 130.17, 130.18, 130.19). A core of swelling (9 cm long) with clear edge is observable at the centre of the thickened area, surrounded by a periostitis area (irregular and remodelled surface, porous or sclerotic aspect due to bony neoapposition, hypervascular imprints. 2) a thickened area focusing on the medial margin (8 cm long), in the distal half of the diaphysis, extending on the antero-medial and posterior faces (Fig. 130.20, 130.21, 130.22).

Fig. 130.7

Fig. 130.8

Fig. 130.9

Fig. 130.10

Fig. 130.11

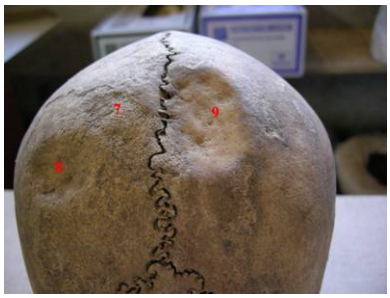

Fig. 130.12

Fig. 130.13

Fig. 130.14

Fig. 130.15

Fig. 130.16

Fig. 130.17

Fig. 130.18

Fig. 130.19

Fig. 130.20

Fig. 130.21

The left tibia shows an extensive thickning (7 cm long) in the distal half of the diaphysis, mostly on the lateral margin, but extending on the antero-lateral and posterior faces, with large areas of roughness, macroporosity or sclerotic neoapposition and with rather clear edges, surrounded by limited periostitis areas (Fig. 130.23, 130.24, 130.25, 130.26, 130.27). Fibulae appear untouched.

Fig. 130.22

Fig. 130.23

Fig. 130.24

Other bones affected:

- Both clavicles, mostly the left one: sternal ends are deeply degenerated with porosity and irregular and widen out edges (Fig. 130.28) The left one shows two gummatous cavities close to the articular surface and opening on this one (Fig. 130.29, 130.30).

- Mandible right condyle (Fig. 130.31, 130.32) has twisted and flattened shape , with porous surface, that does not seem a temporomandibular joint arthritis.

Fig. 130.25

Fig. 130.26

Fig. 130.27

- The distal end of both radii, but mostly the right one, are “swollen” and cribrose , with osteomyelitic appearance ; the distal diaphysis is grooved by vascular imprints (Fig.130.33). On the right one the articular surface also is altered (Fig. 130.34).

- The distal end of the right ulna shows a similar osteomyelitic swelling and alteration (Fig. 130.35). Also the right olecranon (the only observable one) is grossly altered, with irregular surface, deep grooves and porosity (Fig. 130.36, 130.37). Instead, the distal end of the right humerus is undamaged.

Fig. 130.28

Fig. 130.29

Fig. 130.30

Fig. 130.31

Fig. 130.32

Fig. 130.33

Fig. 130.34

Fig. 130.35

Fig. 130.36

Fig. 130.37

Fig. 130.38

Fig. 130.39

Fig. 130.40

Fig. 130.41

Fig. 130.42

- The right carpal bones, as well as the proximal end of the second metacarpal are also “swollen”, festooned, porous; phalanges are undamaged. (Fig. 130.38, 130.39. 130.40, 130.41); the left hand has a similar appearance (Fig. 130.42), but also the proximal end of the first phalanx is affected (Fig. 130.43).
- The left talus and calcaneum (articular surface) (Fig. 130.44, 130.45) and the distal end of the first foot phalanx (Fig. 130.46) are affected, whereas the right foot is undamaged.
- The left auricular surface of ilium has an eroded area (macroporosity) at the angle (Fig.130.47).

In addition to multiple syphilitic lesions, we can observe other pathological features: The cervical vertebrae show arthritis signs both on bodies (festooned edges and porous plates) (Fig. 130.48, 130.49) and on intervertebral facets (some of them are porous and irregularly enlarged) (Fig.130.50, 130.51). The high toracic vertebrae are also affected.

The right femur exhibits the result of a healed fracture of the distal diaphysis, at about 10 cm from the half (Fig.130.52, 130.53, 130.54), with marked longitudinal displacement of the broken ends (about 4 cm overlapping) and angulation on the sagittal plane (the angle is about 30°, convex in front) but very slight mediolateral displacement (angle less than 10 °convex laterally). Callus and post-traumatic ossification are not particularly abundant (Fig.130.55, 130.56, 130.57, 130.58).

Two bony thorns are observable on the lateral and medial side, close to the fracture area, probably due to tendon ossifications. The callus is spangled by a dozen of large holes. Misalignment caused a shortening and a change in the axis of the bone which certainly made trouble in the mechanical function of the lower limb, like uneven locomotion and joint stress.

However joints do not have a degenerated look and the left femur does not show compensative enthesopathy nor marked signs of secondary arthritis at the hip or the knee extremities. This could mean that the individual did not survive for a long time after the trauma. On the other hand, conspicuous development or slight enthesopathy can be observed on muscle insertions of humeri (deltoid, pectoralis major and teres major) (Fig. 130.59) left humerus), radii (biceps and pronator teres) and ulnae (pronator quadratus), besides arthritis signs on glenoids of scapulae, indicating that at least for a period the individual tried to walk on crutches.

Other observations Os acromiale not detectable.

Bilateral asymmetry is detectable in the humerus lengths (right mm 316, left mm 311).

Fig. 130.43

Fig. 130.44

Fig. 130.45

Fig. 130.46

Fig. 130.47

Fig. 130.48

Fig. 130.49

Fig. 130.50

Fig. 130.51

Fig. 130.52

Fig. 130.53

Fig. 130.54

Fig. 130.55

Fig. 130.56

Fig. 130.57

Fig. 130.58

Fig. 130.59

Grave 131

Fig. 131.1

Fig. 131.2

Fig. 131.3

Sex: Male (morphological diagnosis, on the basis of the most discriminant cranial and hip bone features).

Age at death: Mature adult.

Dental wear (maxilla phase H; mandible phase G).

Sutures: coronal open except lateral segments; sagittal in advanced closure, lambdoid in initial closure).

but the pubis symphysis has still a billowing surface (Phase 4) (Fig. 131.4).

Auricular joint has degenerated, sclerotic surface and warped edges (Phase 6) (Fig.131.5).

Stature: Cm 173.

Dental characteristics:

	Right								Left							
	M3	**M2**	**M1**	**P2**	**P1**	**C**	**I2**	**I1**	**I1**	**I2**	**C**	**P1**	**P2**	**M1**	**M2**	**M3**
Maxilla	P	P	P	P	P	P	P	P	P	P	P	P	P	P	P	AM
Mandibula	P	P	P	P	P	P	P	P	P	P	P	P	P	P	P	P

1 small caries on right lower M2 (occlusal, cusp) (Fig.131.6).

Malocclusion: left upper I2 rotation.

Periodontal disease: Slight.

Calculus: Medium.

Shovel shape absent.

Fig. 131.4

Fig. 131.5

Fig. 131.6

Occupational stress indicators and pathological aspects:

Claviculae: entesophatic deltoid; well developed pectoralis major ; severely entesophatic costoclavicular ligament.

Only the right scapula shows evident insertion lines of subscapularis muscle (Fig. 131.7).

Humeri: teres minor entesophatic bilaterally but especially on the left side; teres major bilaterally; pectoralis major on the right side. All the muscle attachments are well developed.

Forearm: muscle attachments are well developed, especially pronator quadratus on ulnae (Fig. 131.8). The right ulna and radio have larger diaphysis then the left ones.

Moreover, bilateral asymmetry in upper limb length (humerus max. length: right mm 351, left mm 345; radio max. length: right mm 247, left mm 244; ulna max. length: right mm 262, left mm 260).

Both radio diaphyses are very curved (lateral convexity) (Look for a possible biomechanical reason).

Hands show sharp edges on metacarpals and well developed insertions for the fibrous flexor sheaths.

All bones have a particularly high weight and density, indicating a considerable bone mass.

Fig. 131.7

Fig. 131.8

Fig. 131.9

Fig. 131.10

Fig. 131.11

Femurs are platimeric; tibiae are platicnemic. Lower limbs are well shaped, show well developed attachments, no enthesopathy, no arthritis signs.

Some small Echinococcus cysts come from the grave, but the provenance district is unknown (Fig. 131.9).

The calcification of the longitudinal anterior ligament is observable like a bridge between L1 and L2, as consequence of vertebral arthritis (Fig. 131.10). Vertebral bodies are well separated and osteophytosis free; osteophytosis is abundant and festooned between L2 and L3; L3 and L4, minor between L4 and L5. This appearance is only involving the superior plates of the vertebrae (Fig. 131.10).

Other observations: Os acromiale absent on both sides.

Many lambdoid ossicles (Fig. 131.11).

Lime deposits are present in form of lumps on the right ribs.

Grave 132

Fig. 132.1

Fig. 132.2

Age at death: Six months, on the basis of teeth development (Fig. 132.2).

Very fragmentary remains. The skull (squama fragments, pyramids), the mandibula and most of the postacranial bones are represented: clavicles, scapulae, right and left ribs, vertebrae, humeri, forearms, hip bones, femurs, tibiae, fibulae, right hand (11 elements), left hand (9 elements). The bones are incomplete and curled up.

Dental characteristics:

	Right					Left				
	m2	**m1**	**c**	**i2**	**i1**	**i1**	**i2**	**c**	**m1**	**m2**
Maxilla	--	P	P	P	--	--	--	--	--	--
Mandibula	--	P	P	P	P	--	P	P	P	P

Grave 133

Fig. 133.1

Sex: Female (morphological diagnosis, on the basis of the most discriminant cranial features).

Age at death: Mature adult. The evaluation tries to balance the following contradictory features:

dental wear is very advanced, exceeding the Lovejoy scale, but sutures are open and vertebral degenerative arthritis signs are absent.

Dental characteristics:

	Right								Left							
	M3	**M2**	**M1**	**P2**	**P1**	**C**	**I2**	**I1**	**I1**	**I2**	**C**	**P1**	**P2**	**M1**	**M2**	**M3**
Maxilla	AG	R	P	AM	AM	AM	P	PM	PM	PM	P	AM	P	P	P	AG
Mandibula	AG	P	P	AM	P	P	P	AM	AM	AM	R	P	P	P	AM	AG

Vestibular abscesses: deep alveolar resorption at upper left M2 (Fig. 133.2) and lower right M1 (Fig. 133.3) and fistula at upper right M1.

Periodontal disease: Medium.

Calculus: Abundant (Fig. 133.3).

Hypoplasia on the canine.

Shovel shape not detectable.

Fig. 133.2

Fig. 133.3

Fig. 133.4

Fig. 133.5

Fig. 133.6

Fig. 133.7

Occupational stress indicators and pathological aspects:

Clavicles are small but the pectoralis major insertion area is very defined and even enthesopathic (Fig.133.4), as well as the deltoid one Fig.133.5).

Humeri have a very large and robust appearance, with deltoid tuberosities highly prominent (Fig. 133.6). Also the pectoralis major insertion is well developed. Slight degenerative arthritis signs (lipping) are detectable on the scapular glenoids (Fig. 133.7).

Other observations: Os acromiale not detectable

Grave 134

Fig. 134.1

Fig. 134.2

Sex: Female (morphological diagnosis, on the basis of the most discriminant cranial and hip bone features).

Age at death: Old.

Dental wear of mandibular posterior teeth is very advanced, exceeding the Lovejoy scale; dental wear of mandibular anterior teeth is phase D. Vertebrae show arthritis signs.

Stature: Not detectable.

Dental characteristics:

	Right								Left							
	M3	**M2**	**M1**	**P2**	**P1**	**C**	**I2**	**I1**	**I1**	**I2**	**C**	**P1**	**P2**	**M1**	**M2**	**M3**
Maxilla	AG	P	P	AM	AM	P	P	--	P	--	P	P	PM	PM	P	P
Mandibula	P	P	P	P	P	P	P	P	P	P	P	P	P	P	P	P

Fig. 134.3

Fig. 134.4

Fig. 134.5

Periodontal disease: Considerable (Fig. 134.3). Alveolar resorption at lower right M2 (Fig. 134.4) and left M2 (Fig. 134.5).

Calculus: Abundant (Fig. 134.3).

Malocclusion: lower anterior teeth crowded, with vestibular dislocation of right P1 and left I1, and rotation of right I2 (Fig. 134.6).

Shovel shape of Upper I1.

Occupational stress indicators and pathological aspects:

The advanced bone erosion prevents to detect most of the indicators. Yet, the forearm muscle insertions appear markedly developed (Fig. 134.7).

Despite of the bad preservation of the column we can observe that 2 cervical vertebrae are affected by the ankylosis of the arches (Fig 134.8).

The cervical vertebrae show arthritis signs, such as porous surface of the intervertebral facets (Fig.134.9, 134.10), besides C5 body is very shortened.

Other observations: Presence of Torus palatinus. Os acromiale not detectable.

Fig. 134.6

Fig. 134.7

Fig. 134.8

Fig. 134.9

Fig. 134.10

Grave 135

Sex: Male: cranial morphological characters; incisura ischiadica major, general robustness and great dimensions.

Age at death: Mature adult. The fine femoral head spongy bone indicates a not old individual, as well as the completely open cranial sutures. But dental wear is quite advanced (maxilla phase H; mandible phase H).

Fig. 135.1

Dental characteristics:

	Right								Left							
	M3	**M2**	**M1**	**P2**	**P1**	**C**	**I2**	**I1**	**I1**	**I2**	**C**	**P1**	**P2**	**M1**	**M2**	**M3**
Maxilla	P	P	P	P	P	P	P	P	PM	PM	P	PM	P	P	P	P
Mandibula	P	P	P	PM	P	P	P	P	P	P	P	P	P	P	P	P

Caries absent.

Malocclusion: crowding: left lower P2 buccal dislocation; left lowerP1 lingual dislocation (Fig. 135.2).

Periodontal disease: Slight.

Calculus: Slight.

Shovel shape: not detectable (Fig. 135.3).

Fig. 135.2

Fig. 135.3

Fig. 135.4

Fig. 135.5

Fig. 135.6

Fig. 135.7

Occupational stress indicators and pathological aspects:

The upper limbs are well shaped, with robust appearance. The right humerus shows a severe enthesopathy of the pectoralis major, while the left one has only a marked attachment of the muscle(Fig. 135.4). Both humeri show enthesopathies of the teres major (Fig. 135.5) and deltoid.

Femurs are platimeric (Index = 82.6) and show marked linea aspra but no enthesopathies. Tibiae show diffuse periostitis on diaphyses (Fig. 135.6). Besides the left one shows a swollen area on the upper half of the medial diaphyseal face, due to osteitis (Fig. 135.7) A X ray would be useful to check the medullary cavity.

Other observations: complete metopism. Presence of Torus palatinus. Os acromiale not detectable

Grave 136

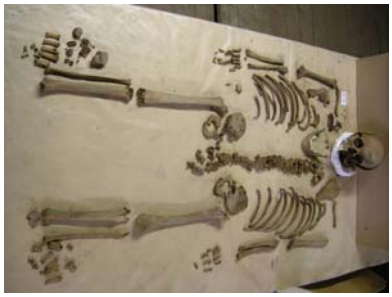

Fig. 136.1

Fig. 136.2

Fig. 136.3

Age at death: 10 years, on the basis of teeth development.

Dental characteristics:

	Right								Left							
	M3	**M2**	**M1**	**m2**	**P1**	**C**	**I2**	**I1**	**I1**	**I2**	**C**	**P1**	**m2**	**M1**	**M2**	**M3**
Maxilla	NE	P	P	P	P	P	P	P	P	P	P	P	P	P	P	NE
Mandibula	NE	P	P	P	P	P	P	P	P	P	P	P	P	P	P	NE

Fig. 136.4

Fig. 136.5

Fig. 136.6

Caries absent.

Calculus: Medium (Fig. 136.4).

Hypoplasia: slight stria at the base of the canine.

Shovel shape: right and left upper I2 (Fig 136.5, 136.6).

Occupational stress indicators and pathological aspects:

Severe enthesopathies can be detected of the deltoid muscle on both clavicles Fig. 136.7) and humeri (Fig. 136.8), of the costoclavicular ligament on the right one (the left one is not detectable) (Fig. 136.9), of the teres major and pectoralis major on both humeri (Fig.136.10), of the biceps on both radii (Fig. 136.11). The complex of these observations indicates a protracted effort on shoulders and arms, probably due to a working activity, e.g. carrying heavy loads (pack-saddle).

Fig. 136.7

Fig. 136.8

Fig. 136.9

Fig. 136.10

Fig. 136.11

The right femur is more curved (the diaphysis is concave behind) and more platymeric than the left one (platymeric index = 82 vs 86).

Grave 141

Fig. 141.1

Fig. 141.2

Not yet cleaned/restored

Age at death: 5 years, on the basis of teeth development (Fig. 141.2).

Only the skull (fragmentary), the mandible and scattered teeth are present.

Dental characteristics:

Permanent	Right								Left							
	M3	**M2**	**M1**	**P2**	**P1**	**C**	**I2**	**I1**	**I1**	**I2**	**C**	**P1**	**P2**	**M1**	**M2**	**M3**
Maxilla	--	NE	--	NE	NE	NE	NE	NE	NE	NE	NE	NE	NE	NE	--	--
Mandibula	--	NE	NE	NE	NE	NE	NE	NE	NE	NE	NE	NE	NE	NE	NE	--

Deciduous	Right					Left				
	m2	**m1**	**c**	**i2**	**i1**	**i1**	**i2**	**c**	**m1**	**m2**
Maxilla	P	P	P	P	P	P	P	P	P	P
Mandibula	P	P	P	P	P	P	P	P	P	P

Grave 142

Age at death: Nine months, on the basis of teeth development.

Teeth are the only findings.

Dental characteristics:

Fig. 142.1

	Right						Left					
	M1	**m2**	**m1**	**c**	**i2**	**i1**	**i1**	**i2**	**c**	**m1**	**m2**	**M1**
Maxilla	NE	P	P	P	P	P	P	P	P	P	P	NE
Mandibula	--	P	P	P	P	P	P	P	P	P	P	NE

Grave 143

Fig. 143.1

Fig. 143.2

Fig. 143.3

Sex: Female, cranial morphological characters; incisura ischiadica major.

Age at death: Mature-old adult. Dental wear is very advanced on molars (exceeding the Lovejoy scale), while it is slight on anterior teeth (phase D on maxilla; phase C on mandible). Advanced vertebral degenerative arthritis and diffuse degenerative arthritis.

Stature: Not detectable.

Dental characteristics:

	Right								Left							
	M3	**M2**	**M1**	**P2**	**P1**	**C**	**I2**	**I1**	**I1**	**I2**	**C**	**P1**	**P2**	**M1**	**M2**	**M3**
Maxilla	AG	AM	P	P	P	AM	P	P	AM	AM	P	P	P	P	P	AG
Mandibula	P	P	P	P	P	P	P	P	P	P	P	P	P	P	P	P

Caries absent.

Periodontal disease: Considerable Fig. 143.4), with particularly advanced alveolar resorption at upper left C, upper right and left M1 and left M2 (Fig. 143.4, 143.5) , lower right I1, lower left M1(Fig. 143.6).

Calculus: Abundant (Fig. 143.4, 143.6).

Malocclusion: Absent.

Shovel shape: Upper I1 and I2.

Fig. 143.4

Fig. 143.5

Fig. 143.6

Occupational stress indicators and pathological aspects:

(Unfortunately diagenetic erosion limits greatly the possibility to detect features). Muscle insertions appear well developed (pectoralis major, dorsalis major and deltoid on right humerus (Fig. 143.7, 143.8); biceps, abductor pollicis longus and pronator teres on right radius (Fig 143.9, 143.10); brachialis and pronator quadratus on ulna. On the femurs, insertions of vastus medialis and linea aspra are enthesopathic (Fig.143.11, 143.12). On the tibiae, insertions of soleus (Fig 143.13).

Vertebral arthritis: in the cervical segment the bodies are severely affected by shortening, porosity of the plates, marginal lipping, exuberant new bone formation along the walls; some diartrodial facets are affected by porosity and irregular enlargement (Fig. 143.14, 143.15); the thoracic segment is not detectable; the 3 lumbar vertebrae are severely affected by osteophytosis and porosity of the plates (Fig. 143.16, 143.17).

Arthritis signs are detectable at the elbows (Fig143.18. 143.19), at the right wrist (Fig. 143.20)

A number of pathologic characters seems referable to the same syndrome as N.145 and N.130, a chronic inflammatory condition, even if to a less extent:

- the distal end of the right ulna shows the periarticular surface grossly porous and swollen (Fig. 143.21), somewhat similar to the individual N.145; also some carpal bones, mostly the scaphoid and capitate of the left side, resemble those of N.145: swollen, perforated, porous, osteophytic and deformed (Fig. 143.22, 143.23);
- the femur head shows a very altered surface, with gross porosity, cavities, sclerosis, remodelling (Fig. 143.24);
- the same appearance can be seen on the humerus head, despite of its incompleteness;
- the right radio shows, on the proximal radio-ulnar joint, a depressed, eroded area (Fig. 143.25);
- the right rotula articular surface shows gross porosity (Fig.143.26);
- finally, the first phalanx of the left foot shows an oval pit with blunted margin, surrounded by remodelled surface, on the proximal joint (Fig. 143.27)

Both tibiae are affected by advanced periostitis on the whole antero-medial face of the diaphysis, with apposition of new bone (Fig. 143.28)

Several ossified Echinococcus cysts and attendant fragments are present, of different dimensions (e.g. Fig. 143.29)

Fig. 143.7

Fig. 143.8

Fig. 143.9

Fig. 143.10

Fig. 143.11

Fig. 143.12

Fig. 143.13

Fig. 143.14

Fig. 143.15

Fig. 143.16

Fig. 143.17

Fig. 143.18

Fig. 143.19

Fig. 143.20

Fig. 143.21

Other observations: Os acromiale not detectable. Presence of Torus palatinus. Four small rounded bumps are detectable on the lingual side of the mandible body, aligned in the space between the right and left premolars Fig. 143.30). The meaning is not clear.

Fig. 143.22

Fig. 143.23

Fig. 143.24

Fig. 143.25

Fig. 143.26

Fig. 143.27

Fig. 143.28

Fig. 143.29

Fig. 143.30

Grave 145

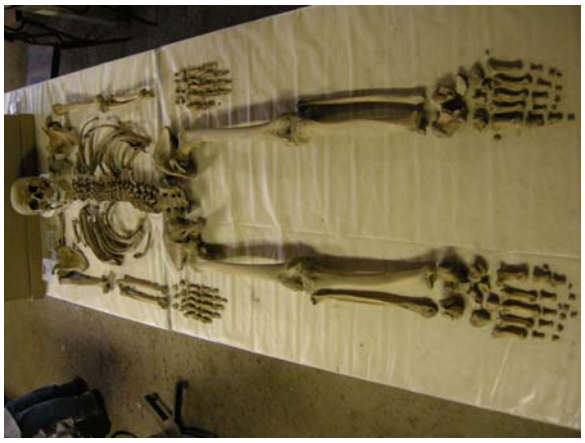

Fig. 145.1

Fig. 145.2

Fig. 145.3

Fig. 145.4

Fig. 145.5

Sex: Male (morphological diagnosis, on the basis of the most discriminant cranial and hip bone features).

Age at death: Mature-old adult. Pubic symphysis has a rather juvenile appearance (Phase 3), but dental wear is advanced: degree more than H for the posterior maxillary teeth; degree H for the anterior ones. Auricular surfaces show granularity but also erosive areas and marginal lipping (Fig. 145.6). Cranial sutures are: the coronal completely closed, the sagittal mostly closed, the lambdoid partly closed. Advanced and diffuse degenerative arthritis is observable. Tyroid cartilage is ossified.

Fig. 145.6

Fig. 145.7

Stature: Cm 161.

Dental characteristics:

	Right								Left							
	M3	**M2**	**M1**	**P2**	**P1**	**C**	**I2**	**I1**	**I1**	**I2**	**C**	**P1**	**P2**	**M1**	**M2**	**M3**
Maxilla	P	P	P	P	P	P	P	P	P	P	P	P	P	P	P	PM
Mandibula	AG	P	P	-	P	-	P	P	P	P	PM	AM	AM	P	P	P

Upper incisors have fractured edge, moreover they are worn almost until the roots.

Periodontal disease: considerable.

Calculus: Abundant (Fig.145.7).

Occupational stress indicators and pathological aspects:

Bones are robust and exhibit scarce enthesopathy. Exceptions are the severely degenerated attachments of subscapularis muscle (more generally the rotator cuff) on both humeri but more evident on the left one (Fig. 145.8), of the biceps on both radii (Fig. 145.9, 145.10).

Vertebral arthritis: in the cervical segment the bodies are affected from C3 to C6, mostly C5, with shortening, porosity and lipping (Fig. 145.11, 145.12); in the thoracic segment the body shortening is asymmetric (T3 on the right side; T5 and T6 on the left side; T7 and T8 on the front part); the T8-T11 piece is the most affected (Fig. 145.13); also the costovertebral joint are affected; the lumbar segment is severely affected, with marginal lipping, erosion, osteophytes development, festooned appearance, longitudinal ligament ossification, body shortening, porotic and broaden diarthrodial facets; the anterior erosion of the adjacent edges of the bodies indicates probably a bony reaction to an anterior herniation of the disk (Fig. 145.14, 145.15). Also the sacrum right diarthrodial facet is sclerotic, porous and broaden (Fig. 145.16).

Many joints are affected by arthritis, more or less severe:

- left elbow shows exuberant marginal lipping and, besides, erosion areas on the articular surfaces of the radio head and humerus capitulum and trochlea (Fig 145.17); the right elbow is normal except the marginal lipping on ulna.
- wrists are also severely affected; the appearance of the periarticular surface is grossly porous and swollen; the joints show marginal lipping , porous or eburnated surfaces and deformation (Fig. 145.18, 145.19, 145.20).
- similar aspects can be observed on left acromion-clavicle joint (Fig.145.21, 145.22), while the glenoid joints of the scapulas are almost undamaged
- hands are both affected: carpal bones have a swollen , perforated, porous, osteophytic and deformed appearance, as so as the metacarpal ends and the proximal end of the proximal phalanges (Fig. 145.23, 145.24, 145.25, 145.26, 145.27).

Fig. 145.8

Fig. 145.9

Fig. 145.10

Fig. 145.11

Fig. 145.12

Fig. 145.13

Fig. 145.14

Fig. 145.15

Fig. 145.16

Fig. 145.17

Fig. 145.18

Fig. 145.19

Fig. 145.20

Fig. 145.21

Fig. 145.22

- hip joints show little marginal lipping but endoarticular signs of cartilage degeneration (porosity areas) (Fig.145.28);
- knees (mostly the left one) show exuberant marginal lipping of femur and tibia; endoarticular new bone apposition on femur; erosive and eburnated areas on tibia (Fig.145.29, 145.30, 145.31);
- tibias show in the metaphysisl medial side, in the area of ligamentum tibialis collateralis attachment, an erosive depression, rounded by a porotic area , whose meaning in not clear (Fig.145.32); the distal epiphyses appear porotic and slightly bulging in the medial side.
- feet are both affected: talus, calcaneum, other tarsal bones, and, on the left side, distal end of the first metacarpus and proximal end of the first phalanx.

On the skull vault an eroded area can be observed on the left parietal bone, 1.5 cm to the sagittal suture and 9 cm to the lambdoid one, with oval shape (cm 1.5x1.0) and sagittal major axis (Fig.145.33). The hole can be of diagenetic meaning, but the photograph taken from inside (Fig. 145.34) let us see a thinning of the bone, not only around the hole but also in other adjacent areas.

A little depressed area is observable close to the left frontal bossing, with irregular margins and pitted bottom (Fig.145.35).

The mandible body is shortened because of the resorption of the alveolar process. A huge and protracted inflammatory process caused resorption, remodelling and swelling, besides the enlargement of the mental foramen (Fig.145.36, 145.37).

Some general considerations can be done about the arthritis disease: it does not seem of degenerative origin, but rather the result of a chronic inflammatory condition, which caused a considerable disruption of many articular surfaces, periarticular reaction and some muscle attachments degeneration.

About the burial deposition in a short coffin, we cannot see a clear anatomical reason, but we can suppose that this may be evidence of rheumatoid deformity without marked bone changes.

Other observations Os acromiale absent on both sides. Lower right M3 agenesis. Lower left M3 reduced. Shovel shape: not detectable.

Bilateral asymmetry is detectable in the humerus lengths (right mm 325, left mm 322).

Fig. 145.23

Fig. 145.24

Fig. 145.25

Fig. 145.26

Fig. 145.27

Fig. 145.28

Fig. 145.29

Fig. 145.30

Fig. 145.31

Fig. 145.32

Fig. 145.33

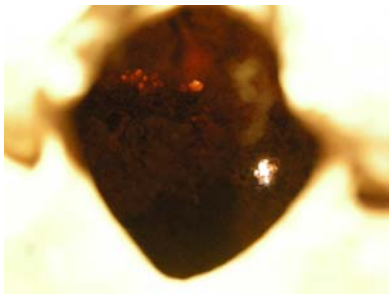

Fig. 145.34

Fig. 145.35

Fig. 145.36

Fig. 145.37

Grave 146

Fig. 146.1

Fig. 146.2

Not yet cleaned/restored

Age at death: Newborn, on the basis of teeth development (Fig. 146.3, 146.4) and some bone length measurements e.g.

Humerus: Diaphyseal length mm57

Transverse diameter at half diaphysis mm 4.5

Transverse width of proximal epiphysis mm 10

Transverse width of distal epiphysis mm 14

Femur: Diaphyseal length mm 66.5

Transverse diameter at half diaphysis mm 6.5

Transverse width of proximal epiphysis mm 15

Transverse width of distal epiphysis mm 19

Fig. 146.3

Fig. 146.4

Some anthropometric measurements in mm (code numbers according Martin and Saller):

	125 M	125 scatt. M	126 F	128 F	129 M	130 M	131 M	135 M	143 F	145 M
1- maximum cranial lenght	-	-	176	173	192.5	172	196	178	181.5	185
8- maximum cranial breadth	-	-	132	128	147	131	140	138	-	142
17- basion/bregma height	-	-	126.5	127	137	131	132	135	133	132
1- maximum humerus lenght	-	-	301	306	313	316	351	-	-	325
2- total humerus lenght	-	-	295	300	309	307	345	-	-	322
7- minimum hum. circumference	-	-	60	60	66	63	67	70	65	68
1- maximum radius lenght	-	-	211	207	227	231	247	-	235	242
3- minimum radius circumference	-	-	41	39	45	42	47	46	43.5	47
1- maximum ulna lenght	-	-	227	224	242	256	262	-	256	254
3- minimum ulna circumference	-	-	37.5	34	36	-	40	47	37.5	40
1- maximum femur lenght	420	476	405	-	427	433.5	480	-	-	426
2- physiological femur lenght	418	474	402.5	-	420	430	475	-	-	425
6- femur sagittal diameter in middle	27	31	25	27	30	27	31	34.5	29	32.5
7- femur transv. diameter in middle	30	30	28	28	30	26.5	32	29.5	30	31
9- femur superior transv. diameter	34	32.5	34.5	29.5	31	32	37	34.5	34	33
10- femur superior sagittal diameter	26	30	22	23.5	27.5	24.5	28	28.5	29	29
1- total tibia lenght	333	-	326	328	334	338	370	-	343	326
8 a – tibia sagittal diameter for nutr	34.5	-	31.5	33	35	32	38	38.5	32.5	36
9 a – tibia transv. diameter for nutr	25	-	24	22	27.5	27.5	26	27	28	29

References

Brooks S. and Suchey J.M., 1990. “Skeletal age determination based on the os pubis: a comparison of the Acsádi-Nemeskéri and Suchey-Brooks methods.” *Human Evolution*, 5:227-238.

Iscan M.Y., Loth S.R., Wright R.K., 1984. “Age estimation from the rib by Phase analysis: white males.” *Journal of Forensic Sciences*, 29, 1094-1104.

Iscan M.Y., Loth S.R., Wright R.K., 1985. “Age estimation from the rib by Phase analysis: white females.” *Journal of Forensic Sciences*, 30, 853-863.

Lovejoy C.O., Meindl R.S., Pryzbeck T.R., Mensforth R., 1985. “Chronological metamorphosis of the auricular surface of the ilium: a new method for the determination of adult skeletal age at death”. *American Journal of Physical Anthropology*, 68:15-28.

Lovejoy C.O., 1985. “Dental wear in the Libben population: its functional pattern and role in the determination of adult skeletal age at death.” *American Journal of Physical Anthropology*, 68: 47-56.

Skýrslur Skriðuklaustursrannsókna

I. Steinunn Kristjánsdóttir 2003: *Skriðuklaustur – híbýli helgra manna. Áfangaskýrsla fornleifarannsókna 2002.* Reykjavík: Skriðuklaustursrannsóknir.

II. Magnús Sigurgeirsson 2003: *Skriðuklaustur í Fljótsdal – fornleifarannsókn 2002. Gjóskulagagreining*. Reykjavík: Skriðuklaustursrannsóknir.

III. Jonathan Møller 2003: *Identification of Skriðuklaustur´s animal bones 2002.* Reykjavík: Skriðuklaustursrannsóknir.

IV. Steinunn Kristjánsdóttir 2004: *Skriðuklaustur – híbýli helgra manna. Áfangaskýrsla fornleifarannsókna 2003*. Reykjavík: Skriðuklaustursrannsóknir.

V. Giuseppe Venturini 2004: *Preservation Condition of Metal Objects From Skriðuklaustur Excavation 2003*. Reykjavík: Skriðuklaustursrannsóknir.

VI. Hákon Jensson 2004: *Garðrækt í Skriðuklaustri*. Verkefni Nýsköpunarsjóðs námsmanna. Reykjavík: Skriðuklaustursrannsóknir.

VII. Albína Hulda Pálsdóttir 2004: *Bókagerð í miðaldaklaustrinu á Skriðu í Fljótsdal*. Verkefni Nýsköpunarsjóðs námsmanna. Reykjavík: Skriðuklaustursrannsóknir.

VIII. Macchioni, Nicola og Lazzeri, Simonia 2004: *Anatomical identification of the wooden samples from the Skriðuklaustur excavation (samples collection summer 2003*). Reykjavík: Skriðuklaustursrannsóknir.

IX. Steinunn Kristjánsdóttir 2005: *Skriðuklaustur – híbýli helgra manna. Áfangaskýrsla Skriðuklaustursrannsókna 2004.* Reykjavík: Skriðuklaustursrannsóknir.

X. Ragnheiður Gló Gylfadóttir 2005: *Miðaldaklaustrið á Skriðu. Leirker.* Reykjavík: Skriðuklaustursrannsóknir.

XI. Steinunn Kristjánsdóttir 2006: *Skriðuklaustur – híbýli helgra manna. Áfangaskýrsla Skriðuklaustursrannsókna 2005*. Reykjavík: Skriðuklaustursrannsóknir.

XII. Þóra Pétursdóttir 2006: *Sjónarhólskofi á Múlaafrétti. – rannsókn og uppgröftur 8.-15. ágúst 2006.* Reykjavík: Skriðuklaustursrannsóknir.

XIII. Dagný Arnarsdóttir 2006: *Miðaldaklaustrið á Skriðu – gerðir líkkistna*. Reykjavík: Skriðuklaustursrannsóknir.

XIV. Pacciani, Elsa 2006: *Anthropological description of skeletons from graves no. 4, 62, 63, 65, 66, 67 and 68 at Skriðuklaustur Monastery*. Reykjavík: Skriðuklaustursrannsóknir.

XV. Steinunn Kristjánsdóttir 2007: *Skriðuklaustur – híbýli helgra manna. Áfangaskýrsla fornleifarannsókna 2006*. Reykjavík: Skriðuklaustursrannsóknir.

XVI. Davíð Bragi Konráðsson 2007: *Bygging Skriðuklausturs*. Verkefni Nýsköpunarsjóðs námsmanna. Reykjavík: Skriðuklaustursrannsóknir.

XVII. Steinunn Kristjánsdóttir 2008: *Skriðuklaustur – híbýli helgra manna. Áfangaskýrsla fornleifarannsókna 2007*. Reykjavík: Skriðuklaustursrannsóknir.

XVIII. Pacciani, Elsa 2008: *Anthropological description of skeletons from graves no. 5, 17, 27, 34, 54, 74 and 75 at Skriðuklaustur Monastery*. Reykjavík: Skriðuklaustursrannsóknir.

XIX. Ragnheiður Gló Gylfadóttir 2008: Skrá yfir leirkerabrot fundin á Skriðuklaustri 2002-2007. Reykjavík: Skriðuklaustursrannsóknir.

XX. Hrönn Konráðsdóttir 2008: *An Archaeoentomological Research of Skriðuklaustur Samples I.*

XXI. Hrönn Konráðsdóttir 2009: *Archaeoentomological analysis of samples from the 2008 season of Skriðuklaustur excavation*. Reykjavík: Skriðuklaustursrannsóknir.

XXII. Pacciani, Elsa 2009: *Anthropological description of skeletons from graves no. 83, 84, 85, 87, 88, 95, 96, 97 and 99 at Skriðuklaustur Monastery*. Reykjavík: Skriðuklaustursrannsóknir.

XXIII. Steinunn Kristjánsdóttir 2009: *Skriðuklaustur – híbýli helgra manna. Áfangaskýrsla fornleifarannsókna 2008*. Reykjavík: Skriðuklaustursrannsóknir.

XXIV. Steinunn Kristjánsdóttir og Margrét Valmundsdóttir 2009: *Kirkja staðarhaldara og sýslumanna á Skriðuklaustri 1554-1793. Áfangaskýrsla um kirkju, grafir og grafsiði*. Reykjavík: Skriðuklaustursrannsóknir.

XXV. Steinunn Kristjánsdóttir 2010: *Skriðuklaustur – híbýli helgra manna. Áfangaskýrsla fornleifarannsókna 2009*. Reykjavík: Skriðuklaustursrannsóknir.

XXVI. Hamilton-Dyer, Sheila 2010: *Skriðuklaustur monastery, Iceland. Animal bones 2003-2007.* Reykjavík: Skriðuklaustursrannsóknir.

XXVII. Collins, Cecilia 2010: *An Osteological Analysis of the Human Remains from the 2009 Excavation Season at Skriðuklaustur, East Iceland.* Reykjavík: Skriðuklaustursrannsóknir.